CLM - P 70

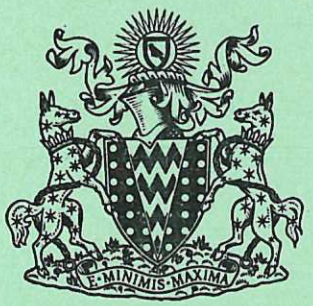

United Kingdom Atomic Energy Authority

RESEARCH GROUP

Preprint

A NUMERICAL STUDY OF PARTICLE BEHAVIOUR IN NON-ADIABATIC MAGNETIC TRAPS

D. A. DUNNETT
E. W. LAING
S. J. ROBERTS
A. E. ROBSON

Culham Laboratory,

Culham, Abingdon, Berkshire

1965

UNCLASSIFIED
(Approved for Publication)

CLM- P 70

A NUMERICAL STUDY OF PARTICLE BEHAVIOUR IN NON-ADIABATIC MAGNETIC TRAPS

by

D.A. DUNNETT *
E.W. LAING*
S.J. ROBERTS
A.E. ROBSON

(Submitted for publication in J. Nucl. Energy Pt C.)

A B S T R A C T

The behaviour of charged particles in a mirror machine with a spatially-modulated central field is examined by adopting a model in which the modulation has the form of a square wave. This enables the equations of motion to be solved algebraically and particle orbits may be computed for long periods in the machine. The non-conservation of magnetic moment allows particles injected through the mirrors to be temporarily trapped, and by considering that mirror reflections randomise the Larmor phase of a particle, a statistical distribution of lifetimes is obtained corresponding to the injection of a beam having a finite spread in initial parameters.

Containment properties are derived for a variety of resonant and non-resonant modulation systems.

*(Department of Natural Philosophy, Glasgow University)

U.K.A.E.A. Research Group,
Culham Laboratory,
Nr. Abingdon,
Berks.

January, 1965 (C/18 MEA)

CONTENTS

TABLES

APPENDIX

1. INTRODUCTION

The containment of charged particles for long periods in a mirror machine generally requires that, in the absence of collisions or collective effects, the magnetic moment of a particle should be an adiabatic invariant. A consequence of this requirement is that particles cannot be accumulated in a stationary mirror field by injection through the mirrors. If however the adiabatic condition is relaxed, so that the magnetic moment may change significantly in one transit of the machine, it becomes possible to trap particles which have been injected through one of the mirrors and to contain them for periods which, although necessarily limited, can be long enough to result in appreciable accumulation of particles in the system. Such an arrangement we call a non-adiabatic magnetic trap.

Although any non-adiabatic effect can result in trapping, the system with which we are principally concerned is one in which particles are injected into a mirror machine along the magnetic lines of force and acquire a large magnetic moment on their first transit due to a resonant interaction with a small, spatially-periodic modulation of the central field. Particles will be lost mainly by the inverse of the capture process, but this does not occur until they have made, on average, an appreciable number of transits between mirrors. This system was first proposed and demonstrated by SINELNIKOV et al (1960 a, b) and some detailed numerical calculations of particle orbits in a trap of this kind were carried out by LAING and ROBSON (1961).

In the latter paper, which we shall refer to as L-R, the model trap consisted of a central field of the form

$$H_z = H_0 \, (1 + h \sin (2\pi z/\lambda)), \text{ where } h \ll 1 ,$$

bounded at each end by adiabatic mirrors. In a typical case, where the modulation consisted of 5 periods with $h = 0.05$, a particle injected along a line of force at a radius λ/π from the axis had 50% of its energy converted into motion transverse to the field when its velocity of injection V satisfied the resonance condition:

$$2\pi V \simeq \frac{eH_0}{mc} \cdot \lambda$$

This particle was then reflected by the end mirror (mirror ratio > 2) and it was shown that the transverse energy could be further increased on the second and third transits by adjustment of the two mirrors so as to reflect the particle back into the modulations with appropriate Larmor phase. The subsequent history of the particle then consisted of variations in transverse energy on successive transits until the magnetic moment was

reduced sufficiently for it to escape through one of the mirrors.

Using step-by-step integration of the equations of motion, orbits should be computed for up to about 25 transits of the system; it was not possible to follow a particle for longer than this without accumulating serious rounding-off errors or using an excessive amount of computer time.

In the present paper we consider a way of overcoming this difficulty by choosing a model magnetic trap in which particle orbits can be calculated algebraically. The sinusoidal modulation considered previously is replaced by a square wave of the same wavelength, consisting of regions of uniform magnetic field having values alternately $H_0 (1 + h)$ and $H_0 (1 - h)$, as shown in Fig.1. Although this system is clearly non-physical on account of the discontinuities in the field, it will be shown that it has closely similar properties to the sinusoidal system. This is because when the characteristic length over which the field varies is already of the order of the Larmor orbit diameter, further reduction in the characteristic length does not significantly alter the effect of the field change on the magnetic moment of the particles. This can be deduced from the calculations of HERTWECK and SCHLUTER (1957) for particles in a time-varying field; their results can be applied to a spatially-varying field by means of a simple transformation.

Using the square-wave model the orbit of a particle can be followed for its entire lifetime in the trap, which may consist of only two transits (the minimum) or may in some cases involve a path in the trap equivalent to many thousand transits between mirrors. The detailed history of a particle is extremely sensitive to small changes in initial conditions: this arises principally through the phase-changing properties of the mirrors. The injection of a beam having a small spread in initial parameters can be simulated by taking the same initial conditions and assuming the mirrors reflect particles with random phase; by computing the orbits of several thousand particles a statistical distribution of lifetimes is obtained, together with information about the density and velocity distributions inside the trap. In this way we have studied the containment properties of a variety of modulation configurations and have attempted to draw some general conclusions on the optimisation of such systems.

2. THE SQUARE WAVE MODEL

As in L-R, we adopt cylindrical co-ordinates in which the model field is now $\underset{\sim}{H} = (0, 0, H_0 f(z))$, where $f(z)$ is the step function $1 + h$, $1 - h$ alternately which replaces the function $1 + h \sin (2\pi z/\lambda)$ used in L-R.

In any region between discontinuities the field is constant, so for region i in which the field is $H_o f_i$ we may write the equations of motion, as derived in L-R,

$$\frac{d^2r}{d\tau^2} = \frac{r_o^4}{r^3} - rf_i^2 \qquad \ldots (2.1)$$

$$\frac{d^2z}{d\tau^2} = 0 \qquad \ldots (2.2)$$

We have used $\tau = \tfrac{1}{2}\omega t$, where $\omega = \frac{eH_o}{mc}$, as a dimensionless time variable. r_o^2 is a constant of the motion proportional to the canonical angular momentum of the particle: physically, r_o is the radius at which the particle has zero mechanical angular momentum, which is identical with the radius of injection .

A first integral of (2.1) and (2.2) gives the energy equation

$$\left(\frac{dr}{d\tau}\right)^2 + \left(\frac{dz}{d\tau}\right)^2 + \left(\frac{r_o^2}{r} - rf_i\right)^2 = v^2 \qquad \ldots (2.3)$$

where the parameter v is the second constant of the motion and is related to the total velocity V of the particle by $V = \tfrac{1}{2}\omega v$.

The general solution of (2.1) is

$$r^2 = \alpha_i + \beta_i \cos(2f_i\tau + \varphi_i) \qquad \ldots (2.4)$$

where

$$\alpha_i^2 - \beta_i^2 = \frac{r_o^4}{f_i^2} \qquad \ldots (2.5)$$

At any time the state of the particle is adequately described by only two parameters, α_i and the phase $2f_i\tau + \varphi_i$.

Physically,

$$r^2 = r_G^2 + r_L^2 + 2r_G r_L \cos(2f_i\tau + \varphi_i)$$

with r_G and r_L the guiding centre radial co-ordinate and the Larmor radius respectively, (Fig.2), so that

$$\alpha_i = r_G^2 + r_L^2 \quad \text{and} \quad \beta_i = 2r_L r_G$$

At a discontinuity in the field, r and $\frac{dr}{d\tau}$ will be continuous, the latter since the effect of the discontinuity is a singular radial field, which does not affect motion parallel to it. Thus applying continuity of r^2 and $\frac{dr}{d\tau}$ across the boundary between region i and region $i+1$ we have,

$$\begin{aligned} \alpha_i + \beta_i \cos\varphi_i &= \alpha_{i+1} + \beta_{i+1} \cos\psi_{i+1} \\ f_i\,\beta_i \sin\varphi_i &= f_{i+1}\,\beta_{i+1} \sin\psi_{i+1} \end{aligned} \qquad \ldots (2.6)$$

where we have put $\tau = 0$ at the boundary and have used ψ and φ for the phase of a particle at the beginning and the end respectively of the region denoted by the subscript. These are related by

$$\varphi_i = \psi_i + \theta_i \qquad \ldots (2.7)$$

where the phase change θ_i is given by

$$\theta_i = \frac{2\ell_i f_i}{u_i} \qquad \ldots (2.8)$$

Here ℓ_i is the axial length of region i and $u_i = (\frac{dz}{d\tau})_i$. The quantity u_i can be derived from (2.3) and (2.4).

Introducing

$$(\eta_i, \zeta_i) = \beta_i (\cos \psi_i, \sin \psi_i)$$

$$\sigma_i = \alpha_i + \eta_i \cos \theta_i - \zeta_i \sin \theta_i$$

we obtain

$$\zeta_{i+1} = \frac{f_i}{f_{i+1}} (\eta_i \sin \theta_i + \zeta_i \cos \theta_i)$$

$$\eta_{i+1} = \tfrac{1}{2}\left(\sigma_i - \frac{1}{\sigma_i}(\zeta_{i+1}^2 + \frac{r_o^4}{f_{i+1}^2})\right) \qquad \ldots (2.9)$$

and thus, using (2.5)

$$\alpha_{i+1} = \tfrac{1}{2}\left(\sigma_i + \frac{1}{\sigma_i}(\zeta_{i+1}^2 + \frac{r_o^4}{f_{i+1}^2})\right) \qquad \ldots (2.10)$$

This enables us to calculate α_{i+1} from α_i and the phase change θ_i. Thus, given the initial conditions, we can compute the trajectory of the particle through the modulations.

An important parameter by which we describe the state of the particle is the normalised magnetic moment ξ given by

$$\xi = \frac{v_\perp^2}{v^2} = 1 - \frac{\left(\frac{dz}{d\tau}\right)^2}{v^2}$$

This can be derived from α_i using (2.3), giving

$$\xi_i = \frac{2f_i}{v^2}(\alpha_i f_i - r_o^2)$$

After n periods of modulation (consisting of $2n$ regions) we have $f = 1$ and

$$\xi = \frac{2}{v^2}(\alpha_{2n+1} - r_o^2)$$

The reciprocal of this quantity gives the mirror ratio required to reflect the particle.

We now compare the square wave and the sine-wave models by computing ξ as a function of v for the first transit. Following the convention used in L-R we take the modulation wavelength as 2π so that all the ℓ_i's are equal to π. The resonance condition is therefore $v \approx 2$.

The initial conditions for a particle injected along the field are

$$\alpha_o = r_o^2 \ , \ \varphi_o = o, \ (\frac{dz}{d\tau})_o = v \ , \ f_o = 1$$

The only adjustment needed to match the two models is in the value of h. It is shown in the Appendix that for vanishingly small h, equal values of ξ are obtained when $v = 2$ if

$$h_{\text{square-wave}} = \frac{\pi}{4} h_{\text{sine-wave}} \qquad \ldots (2.11)$$

The ξ-v resonance curves which are obtained using this relation are given in Fig.3; it can be seen that there is close agreement between the two models.

3. FIRST TRANSIT

For a particle injected along the field lines into a modulation of given n, the magnetic moment ξ_1' acquired on the first transit is a function of v, h, and r_o. It is convenient to take r_o = constant and to plot ξ_1' as a function of v and h. The results can then be presented as a map with contours of constant ξ_1' projected on to the v-h plane. This is done in Fig.4 for the case $n = 5$; the area shown is the region of the main resonance, $v \approx 2$. Alternatively we can take h = constant and plot ξ_1' as a function of v and r_o. The resulting map is closely similar to Fig.4, which is to be expected since the perturbation theory given in the Appendix shows that ξ_1' is a function of the production hr_o.

It can be seen that ξ_1' has a resonance both with respect to v and, for large ξ_1' with respect to h (and r_o) as well. The significance of the v resonance is obvious; the r_o resonance corresponds to spatial selectivity of injection radius, and arises from the non-linearity of the system.

In what follows we decide the injection conditions by selecting a particular value of ξ_1' and, with r_o = constant, choosing from the ξ_1'-h-v diagram the minimum value of h which will produce it, thereby also fixing v. This procedure will be justified in Section 7.

4. SUBSEQUENT TRANSITS

If a particle which has acquired $\xi = \xi_1'$ on its first transit passes into an adiabatic mirror of ratio R it will be reflected provided $\xi_1' > 1/R$, and will return to the modulations with the same ξ but with a Larmor phase φ which depends on its detailed path in the mirror. The state of a particle at any point can be adequately described by the two parameters ξ and φ. A transit through the modulations changes both ξ and φ; a reflection from a mirror changes φ only. We can therefore define transfer functions F_1, F_2, F_3, such that

$$\xi_m' = F_1(\xi_m, \varphi_m)$$
$$\varphi_m' = F_2(\xi_m, \varphi_m) \qquad \ldots (4.1)$$

represent the effect of the modulations, and

$$\varphi_{m+1} = F_3(\xi_m', \varphi_m') \qquad \ldots (4.2)$$

together with

$$\xi_{m+1} = \xi_m$$

represent the effect of a mirror, where (ξ_m, φ_m) and (ξ_m', φ_m') are the states of the particle at the beginning and end respectively of the m^{th} transit.

Thus starting with the initial state $(0,0)$ we may compute the history of a particle by successive application of (4.1) and (4.2); the particle is lost from the trap if at any stage ξ' falls below the value $1/R$.

Given the modulation structure (n,h) and the constants of the motion of the particle (r_0, v), F_1 and F_2 may be constructed by computing particle orbits in the manner described in Section 2. F_1 may then be presented as a map in which contours of constant ξ' are projected on the (ξ,φ) plane. In Fig.5 this is done for $n = 5$, $h = .042$ and $r_0 = 2$, $v = 2.21$. As can be seen from Fig.4 this combination of parameters will give $\xi_1' = 0.5$. Only contours of ξ' up to 0.5 are shown; above this value patterns of great complexity result which are not conveniently represented in this way.

Only the reverse transit is shown in Fig.5. A complete description of F_2 requires two maps, since in general the function will be different for forward and reverse transits (we define a transit as forward if it is in the direction of injection). For a system in which all the ℓ_i's are equal, the difference is small and arises because a particle first encounters an upward field step on a forward transit and a downward field step on a reverse

transit (Fig.1). If the modulations are made symmetrical by adding an additional half-period only one map is required for both directions.

Since the F_1 maps give a complete description of the action of the modulations in changing ξ it is appropriate to compare the results from the square-wave model with a similar map obtained from the sine-wave model. Fig.6 shows a reverse transit map for a sine-wave system with $n = 5$, $h = .05$ and $r_o = 2$, $v = 2.15$. This combination of parameters gives $\xi_1' = 0.475$ and although not exactly equivalent to the case of Fig.5 the general similarity of the maps illustrates the correspondence of the two models.

The important region of these maps is where ξ' is small; for emphasis the contour $\xi' = 0.1$ is shown thicker than the rest. A particle which at any stage enters the modulations with (ξ,φ) falling within this contour will be lost after that transit if the mirror ratio is less than 10. The $\xi' = 0.1$ valley projects from below the line $\xi = 0.1$ to above the line $\xi = 0.5$, so that for any value of $\xi < 0.5$ there is a certain band of phases for which a particle will be lost.

In Figs.5 and 6 the contours $\xi' = 0.033$ and $\xi' = 0.01$ are also shown, corresponding to 'escape valleys' with mirror ratios of 30 and 100 respectively. As the mirror ratio increases these contours shrink towards a singular point $\xi' = 0$, which represents the only escape route when the mirror ratio is infinite. It lies on the line $\xi = \xi_1'$ and corresponds to a particle taking exactly the inverse path to its original resonant capture orbit.

The function F_2 which determines the phase of a particle after passage through the modulations can be derived in a similar fashion to F_1, but we shall not do this here as it does not reveal features of fundamental interest.

5. INTERNAL REFLECTIONS

When calculating the orbit of a particle through the modulations, it sometimes happens that at a particular discontinuity the value of ξ_{i+1}, as derived from ξ_i by the methods of section 2, is greater than unity. Since $\xi > 1$ is forbidden by the conservation of energy, this indicates that the particle cannot enter region $i+1$, and is reflected at the field step. We term this event an internal reflection. Whereas adiabatic reflection is a consequence of the conservation of energy and the invariance of the magnetic moment, reflection at a field step arises from the conservation of energy and of canonical angular momentum. The condition for reflection depends on both ξ_i and the phase φ at the field step, and the range in (ξ,φ) over which reflection occurs is shown in Fig.7 for single

field steps $1-h \to 1+h$, and $1+h \to 1-h$, with $h = 0.039$. It can be seen that reflection can occur in both cases, but over a smaller range of (ξ,φ) for a step in which the field decreases. Also, for $\xi \to 1$ there is a range of phase for which a particle will be transmitted, even through a step of increasing field.

Also shown in Fig.7 is the range of (ξ,φ) over which reflection occurs at a field transition given by

$$H = 1 \pm h \cos z$$

where the orbits are now computed by numerical integration between $z = 0$ and $z = \pi$, and $h = 0.05$ according to the scaling relation (2.11).

In contrast to the results for the discontinuous step all particles with sufficiently large ξ are reflected by the increasing field. At $\xi = \frac{1-h}{1+h}$, which is the value for adiabatic reflection, reflection occurs over half the phase range. For a decreasing field step, there is no reflection. In addition, when reflection occurs at a discontinuity, ξ is unchanged, but upon reflection from the cosine step ξ undergoes a change dependent on phase.

Thus although internal reflections can occur in both the square-wave and the sine-wave cases, there are detailed differences in the predictions of the two models.

6. PHASE RANDOMISATION AT THE MIRRORS

To derive the function F_3 which determines the phase with which a particle returns to the modulations after reflection at a mirror, we consider a mirror described by the expression:

$$H = H_0 \left(1 + \frac{R-1}{2} (1 - \cos \frac{\pi z}{L})\right) \qquad \ldots (6.1)$$

where R is the mirror ratio and L the distance between the minimum and maximum of the field. Using the method given in L-R we derive the phase change in this mirror:

$$\varphi_{m+1} - \varphi'_m = \frac{8L}{\pi v \xi^{\frac{1}{2}} (R-1)^{\frac{1}{2}}} \left[R \cdot K(k) - (R-1) \cdot E(k) \right] \qquad \ldots (6.2)$$

where

$$k = \left(\frac{\frac{1}{\xi} - 1}{R - 1} \right)^{\frac{1}{2}}$$

and $K(k)$ and $E(k)$ are the complete elliptic integrals of the first and second kind respectively.

It follows from (6.2) that a group of particles having phase φ'_m and a small spread in magnetic moment between ξ and $\xi+\delta\xi$ will acquire on reflection a spread in phase given by

$$\delta\varphi_{m+1} = \frac{4L\delta\xi}{\pi v} \cdot \frac{1}{\xi^{3/2}(R-1)^{1/2}} \left\{ (R-1)\left(1 - \frac{1}{\xi(1-\xi)(R-1/\xi)}\right) E(k) - \left(R - \frac{1}{1-\xi}\right) K(k) \right\} \quad \ldots (6.3)$$

Taking typical values $R = 4$, $\xi = 0.5$, $v = 2$, we derive that $\delta\varphi_{m+1}$ will be greater than 2π if

$$L\delta\xi > 0.25\pi \quad \ldots (6.4)$$

Putting $L = 5$, which is, in our units, the length for which a mirror of the above form will reflect particles adiabatically (GARREN et al, 1958), we find that a spread $\delta\xi = .05$ will result in φ being completely spread through 2π.

A beam of particles injected into the trap will acquire a small spread in ξ on their first transit, due to the spread in initial parameters (r_o, v). For the case we have been considering a spread $\delta r_o = 0.1$ $(r_o = 2)$ will result in $\delta\xi'_1 = 0.05$ $(\xi'_1 = 0.5)$ and so ensure complete phase spreading on the first reflection. We see from Fig.5 that on the reverse transit the spread in phase will have a far greater dispersive effect on ξ'_2 than the spread $\delta\xi_2$, and after this transit the particles will all take widely different paths through the system. At each successive passage through the modulations there will be a further dispersion in ξ, brought about mainly by the phase-spreading properties of the mirrors at each reflection.

In order to calculate the average behaviour of a group of particles with a small random spread in initial parameters it seems therefore legitimate to start each particle with the same initial conditions, but to randomise its phase at each reflection*. The model is then independent of the shape of the mirror field and F_3 becomes a random number between 0 and 2π.

7. PARTICLE CONTAINMENT

Starting from the same initial conditions (r_o, v), we use exact calculations for F_1 and a random number generator for F_3 and obtain a statistical distribution of lifetimes in the trap by computing the orbits of, typically, 1000 particles at a time. To keep the results independent of the length and shape of the mirrors we count only the time spent in

---

* A similar suggestion has been put forward by GRAD and VAN NORTON (1962) for slightly non-adiabatic orbits in cusp geometry.

the central, modulated region and normalise the time to τ_o, the time a particle would take to transverse this region if all its energy were in motion along the field. Thus

$$\tau_o = \sum_1^{2n} \frac{\ell_i}{v} \qquad \ldots (7.1)$$

which for the system we are considering, with all ℓ_i's equal to π, is

$$\tau_o = \frac{2n\pi}{v} \qquad \ldots (7.2)$$

The normalised mean lifetime T thus obtained is then the ratio of the line density of particles in the trap to the line density in the injected beam.

For our first case we take a system $n = 5$, $h = 0.042$ and choose initial injection conditions $r_o = 2$, $v = 2.19$. From Fig.4, these particles acquire $\xi_1' = 0.5$ on the first transit. The distribution of containment times is presented in histogram form in Fig.8 for two values of mirror ratio, $R = 10$ and $R = 100$ respectively. The histograms are plotted logarithmically with respect to time in order to show the main features of the distribution: at the smaller mirror ratio a large fraction of the particles is lost in the first few transits ($\tau < 10$) but there is a long tail extending out to $\tau = 1000$ with a pronounced maximum in the region of $\tau = 100$. The mean lifetime T in this case is 31. For the larger mirror ratio the initial loss is greatly reduced and the maximum correspondingly enhanced: the mean lifetime is 100. The heavy initial loss with $R = 10$ can be qualitatively predicted by noting the size of the escape region ($\xi' < 0.1$) in Fig.5. The maximum in the tail is attributed to particles having achieved sufficiently large ξ to undergo internal reflections, which enhance their lifetime.

The statistical accuracy of the mean lifetime was checked by performing 5 runs of 1000 particles each: the standard deviation was 8%. To check the validity of our assumption of phase randomisation we performed two further runs of 1000 particles in which the phase was randomised only at the first reflection and thereafter calculated exactly using (6.2) with $R = 10$ and $L = 10$. The results were within the standard deviation of the previous runs.

The variation of T with mirror ratio, other parameters being kept constant, is shown in Fig.9. It can be seen that T is relatively insensitive to R below $R = 10$, but then increases nearly linearly with R. The relationship in the latter region is given quite closely by

$$T = 2.63\, R^{0.94} \qquad \ldots (7.3)$$

The increase in T coincides with the contraction of the size of the escape hole in (ξ,φ) space towards the singular point $(\xi' = 0)$; T is approximately inversely proportional to the area of the escape region on the (ξ,φ) map.

To investigate the variation of T with small variations in v and h we chose from Fig.4 several points for which the (v,h) combination gave $\xi_1' = 0.5$ and performed containment calculations with R = 10. For increased accuracy we took 5000 particles in each run: the results are shown in Fig.10 as numbers on the $\xi_1' = 0.5$ contour. It can be seen that T is largest for the smallest values of h and v.

The above results all suggest that the containment of particles in a non-adiabatic trap may be regarded as a diffusion in (ξ,φ) space from a source at $\xi = \xi_1'$ to a loss boundary at $\xi = \frac{1}{R}$. Randomisation of phase represents complete diffusion in the φ-direction at each mirror reflection; each transit of the modulation results in diffusion in the ξ-direction, with a step which, as we would expect from perturbation theory, is larger the larger h. With source and sink fixed the mean containment time should increase with decreasing h: this is found to be the case (Fig.10) and so justifies the method of choosing h and v used in Section 3.

The effect of varying ξ_1', adjusting v in each case to minimise h, is shown in Table 1. As ξ_1' is varied from 0.3 to 0.7, T goes through a broad maximum. At small ξ_1', T is reduced because of the larger fraction escaping on the first reverse transit. For large ξ_1', although particles are initially trapped into more highly contained orbits, h is larger and the escape region is also extended into the region of high ξ, so the area of (ξ,φ) space available for containment is decreased.

An important by-product of these calculations is the steady-state distribution of particles in ξ-space. By accumulating the time a particle spends in the range ξ to $\xi + \delta\xi$ and normalising to the mean containment time T, we obtain a typical distribution shown in histogram form in Fig.11. Also shown dotted in this diagram is an isotropic distribution in velocity space: it can be seen that the distribution in the trap is somewhat enhanced in the regions of high ξ and we attribute this to the occurrence of internal reflections.

In an attempt to assess the importance of internal reflections on containment we carried out calculations in which internal reflections were artificially suppressed: this was done by ignoring the time a particle spends between an internal reflection and its

subsequent entry into a mirror. For our typical case (Fig.8) the mean containment at R = 10 was reduced from 30 to 20 and the hump in the containment histogram around $\tau = 100$ disappeared. Thus in this case particles which suffer internal reflections make a very significant contribution to the mean containment, and it is in this respect that the predictions of the square-wave model might differ from what would be observed in a more physically realisable system, due to the detailed differences in the nature of the internal reflections discussed in Section 5. However, a discussion of this point is not within the scope of this paper and in what follows the effect of internal reflections will be included.

8. VARIATION OF THE NUMBER OF MODULATION PERIODS

We have examined a number of configurations with different n, choosing h and v in each case to give $\xi_{\cdot}' = 0.5$. The results are shown in Table 2. As n is increased h can be decreased (we should expect nh = constant from perturbation theory) and T arises approximately linearly with n up to n = 12. As n goes to 15, T decreases, as now the non-linearity of the system requires that h must be increased to achieve the same $\xi_{\cdot}'$.

An increase in n is accompanied by increased selectivity of input conditions and a reduction in the size of the escape region. For example, we show in Fig.12 the initial resonance diagram for n = 10, and in Fig.13 the reverse transit F_1 map for this system. These figures should be compared with Figs.4 and 5, which refer to n = 5.

9. STAGGERED MODULATIONS

The decrease in axial velocity which accompanies the increase in ξ on the first transit makes it impossible to preserve exact resonance throughout the system if all the ℓ_i's are equal and the effect of this non-linearity is particularly apparent at large n. An obvious way of overcoming this difficulty is to arrange that the modulation wavelength decreases progressively to keep the field discontinuities in step with the Larmor rotation of the particle. It can be shown that the phase change θ_i in each section must be π, so that each ℓ_i is given by

$$\ell_i = \frac{\pi u_i}{2f_i} \quad \text{where} \quad u_i = \left(\frac{dz}{d\tau}\right)_i \qquad \ldots (9.1)$$

Taking v = 2, $r_o = 2$, and a given value of h, we construct the modulation system by calculating the first transit orbit in the manner of Section 2, applying (9.1) to

determine the length of each region. For given h and n, the effect of staggering is to reach a larger value of ξ_1' than in the non-staggered case: alternatively, to reach a given ξ_1' the h required is now smaller.

As before we take $\xi_1' = 0.5$, and construct systems with n from 3 to 15. The results of containment runs of 1000 particles in each of these systems are given in Table 3. It can be seen that the containment time T for each value of n is less than for the corresponding case with non-staggered modulations, even though h has been significantly reduced. The reason is apparent from an examination of the F_1 maps. The maps for $n = 10$ are shown in Fig. 14. Two maps are necessary because forward and reverse transists are now significantly different. The main anti-resonance occurs on the reverse transit where the size of the escape region $\xi' < 0.1$ is now appreciably larger than in the non-staggered case (cf Fig. 13). There is also a large escape region in the forward transit, although it does not extend above $\xi = 0.4$.

The range of input conditions over which particles are captured is increased by staggering the modulations. The (ξ', h, v) map for the first transit with $n = 10$ is shown in Fig. 15 and should be compared with the corresponding map for uniform modulations in Fig. 12. However, our containment results apply only over the small range of input conditions (r_o, v) which produces a 10% spread about the chosen value of ξ_1' (from Section 6 this gives phase randomisation at the first mirror reflection). For both the non-staggered and staggered systems the range $\frac{\delta r_o}{r_o} \approx 5\%$, as can also be deduced from the perturbation theory given in the Appendix.

10. NON-ZERO ξ_1

So far we have only considered injection of particles along the field $(\xi_1 = 0)$. Clearly ξ_1 may have any value up to $1/R$, and with non-zero ξ_1, it might be expected that the value of h could be reduced. However, with non-zero ξ_1 the value of ξ_1' depends on the input phase, and since the injected beam has to traverse the first mirror before reaching the modulations the considerations of Section 6 apply: we must therefore assume that all input phases are present so ξ_1' will have a substantial spread of values. In Fig. 16 we show the maximum and minimum values of ξ_1' as a function of h, for $\xi_1 = 0.1$ and $n = 5$. For small h the spread in ξ_1' is practically symmetrical about ξ_1, and so with a mirror ratio of 10 about half the injected particles are lost on the first transit. At $h = 0.035$ however, all particles have $\xi_1' > 0.1$ and are trapped, but h is not

significantly different from when $\xi_1 = 0$; a containment run with 1000 particles gave $T = 19.2$. Thus it appears that if all particles are still to be trapped, injection with non-zero ξ_1 has no advantage over injection along the field.

11. VERY LONG LIVED PARTICLES AND SMALL h

For $h < 0.035$ in the previous example, a fraction of the injected particles is not captured on the first transit. To see whether this disadvantage could be offset by increased containment of the trapped particles we performed 1000-particle containment runs with h down to 0.005. The statistical accuracy of these runs was very bad and this was found to be due to the presence of a few very long lived particles which had a profound effect on the mean containment time. From Tables 1-3 it can be seen that as h decreases, the fraction of particles undergoing internal reflections decreases, but the number of internal reflections per particle increases. Table 5 summaries the results of two runs with $h = 0.01$ in which there is only one internally reflected particle in each group of 1000; in the second case this has a lifetime of 85,932.

The very long life of this particle was not due to its being trapped exclusively in one of the modulation regions since a normalised spatial distribution, obtained as a by-product of the calculation in a similar manner to the normalised velocity distribution, did not show any local increase in density. It seems rather that this particle is one that has reached a very high ξ by diffusion in ξ-space and the occurrence of internal reflections is simply an indication of this.

To obtain statistically significant mean lifetimes for this case we should have to perform containment runs for several hundred thousand particles and such calculations are beyond the scope of this work.

12. STOCHASTIC TRAPPING

For small h and $\xi_1 = 1/R$ we see from Fig.16 that the spread in ξ_1' causes about half the particles to be lost on the first transit: the necessity for a resonant perturbation is now questionable, since a similar spread is produced by any small non-adiabatic effect. We therefore consider as our final example a system with only two field steps (Fig.17) and take the distance between the steps to be sufficiently large that we can apply the concept of phase randomisation at each step: this system we call a stochastic trap and could represent a mirror machine with slightly non-adiabatic mirrors. Results of

containment runs at different h are summarised in Table 5, for $R = 10$ and $\xi_1 = 0.1$. As might be expected, as h decreases T increases, while the spread $\xi_1'_{max} - \xi_1'_{min}$ on the first transit decreases. We can take $\delta\xi = \xi_1 - \xi_1'_{min}$ as the width in ξ-space of an injected beam for which all the particles have a chance of capture. The most significant result is that the product $T\delta\xi$ appears to be constant within the accuracy of our calculations, so that the particle density in the trap is proportional to the beam density in ξ-space irrespective of the value of h.

In order to compare stochastic and resonant trapping, consider a beam with radius $r_o = 2$ and width $\frac{\delta r_o}{r_o} = 5\%$, initially having $\xi = 0$. If this beam is injected into a resonant trap the best value of T we have found is 80 (Table 2). If, however, the same beam were to acquire $\xi_1 = 0.1$ by being passed through a simple resonant system before injection into a stochastic trap, the spread $\delta\xi_1/\xi_1 \approx 10\%$, and the minimum h which would give all particles a chance of capture is slightly less than 0.01. The T for the entire beam is then about half the T for $\xi_1 = 0.1$, (Table 5) that is about 200.

13. CONCLUSIONS

The use of the square wave model allows us to calculate the orbits of large numbers of particles in non-adiabatic traps and to build up a statistical picture of containment. Although resonant trapping enables all injected particles to be caught on the first transit, containment is limited by the anti-resonant escape process; we find that in spite of heavy initial losses, stochastic trapping appears to offer greater possibilities for particle accumulation than resonant trapping. However, very long lived particles appear in calculations on resonant trapping with very small h, but unfavourable statistics prevent any general conclusion being drawn in such cases.

Where we have compared the behaviour of particles in fields which change discontinuously and fields which vary sinusoidally over a distance of the order of a Larmor diameter we find close correspondence except for particles of such large ξ that reflection is possible at the field change. There are then some differences in behaviour which may affect the quantitative accuracy of some of the containment results but which do not affect the general conclusions of this work.

14. REFERENCES

GARREN, A., et al. (1958). Proceedings of the Second International Conference on Peaceful uses of Atomic Energy,Geneva, 31, 65. United Nations, N.Y.

GRAD, H., and VAN NORTON, R., (1962), Nuclear Fusion, 1962 Supplement, Part 1, 61.

HERTWECK, F., and SCHLUTER, A., (1957). Z. Naturf., 12a, 844.

LAING, E.W., and ROBSON, A.E., (1961), J. Nucl. Energy Part C, 3, 146.

SINELNIKOV, K.D., et al. (1960a), Zh. Tekh. Fiz., 30, 249; Soviet Phys.-Tech. Phys., 5, 229.

SINELNIKOV, K.D., et al. (1960b) Zh. Tekh. Fiz., 30, 256; Soviet Phys.-Tech. Phys., 5, 236.

TABLE 1

EFFECT OF VARYING ξ_1' IN UNIFORM MODULATION SYSTEM

R = 10, n = 5, 5000 PARTICLES

ξ_1'	0.3	0.4	0.5	0.6	0.7
v	2.09	2.13	2.19	2.29	2.40
h	0.029	0.035	0.042	0.050	0.064
MEAN CONTAINMENT TIME T	17.7	33.9	31.3	32.2	22.4
AVERAGE NUMBER OF MIRROR REFLECTIONS PER PARTICLE	9.1	15.1	13.7	13.8	10.4
PERCENTAGE OF PARTICLES LOST AFTER FIRST REVERSE TRANSIT	43.6	32.4	21.8	18.0	21.8
PERCENTAGE OF PARTICLES INTERNALLY REFLECTED	2.4	12.2	20.2	51.6	65.5
AVERAGE NUMBER OF INTERNAL REFLECTIONS PER PARTICLE	154	84	57	27	17

TABLE 2

EFFECT OF VARYING n IN UNIFORM MODULATION SYSTEM

R = 10, ξ_1' = 0.5, 1000 PARTICLES

n	3	5	7	10	12	15
v	2.16	2.21	2.24	2.26	2.25	2.19
h	0.064	0.042	0.033	0.030	0.026	0.043
MEAN CONTAINMENT TIME T	22	27	42	61	80	42
AVERAGE NUMBER OF MIRROR REFLECTIONS PER PARTICLE	10	12	18	26	35	18
PERCENTAGE OF PARTICLES LOST AFTER FIRST REVERSE TRANSIT	33.4	27.5	19.1	10.3	8.8	18.5
PERCENTAGE OF PARTICLES INTERNALLY REFLECTED	42	19	16	17	14	37
AVERAGE NUMBER OF INTERNAL REFLECTIONS PER PARTICLE	15	53	106	180	312	133

TABLE 3

EFFECT OF VARYING n IN STAGGERED MODULATION SYSTEM

$R = 10$, $\xi_1' = 0.5$, 1000 PARTICLES

n	3	5	7	10	15
v	2	2	2	2	2
h	0.058	0.035	0.025	0.017	0.012
MEAN CONTAINMENT TIME T	25	29	35	42	49
AVERAGE NUMBER OF MIRROR REFLECTIONS PER PARTICLE	11	13	15	19	22
PERCENTAGE OF PARTICLES LOST AFTER FIRST REVERSE TRANSIT	37.0	32.4	25.5	23.7	16.9
PERCENTAGE OF PARTICLES INTERNALLY REFLECTED	36	22	15	9.5	4.4
AVERAGE NUMBER OF INTERNAL REFLECTIONS PER PARTICLE	20	40	71	125	326

TABLE 4

RESULTS OF TWO 1000 PARTICLE RUNS, EACH WITH ONE INTERNALLY REFLECTED PARTICLE.

$n = 5$, $h = 0.01$, $r_o = 2$, $v = 2.05$, $R = 10$, $\xi_1 = 0.1$

	FIRST RUN	SECOND RUN
T FOR 1000 PARTICLES	31.5	100.8
T FOR 999 PARTICLES	13.6	14.9
LIFETIME OF INTERNALLY REFLECTED PARTICLE	17,945	85,932
NUMBER OF INTERNAL REFLECTIONS	2,460	12,194

TABLE 5

EFFECT OF VARYING h IN STOCHASTIC TRAP

$v = 2$, $r_0 = 2$, $R = 10$, $\xi_{\perp} = 0.1$. 5000 PARTICLES

h	0.04	0.03	0.02	0.01
MEAN CONTAINMENT TIME T	119	148	200	413
AVERAGE NUMBER OF MIRROR REFLECTIONS PER PARTICLE	55	68	92	195
PERCENTAGE OF PARTICLES LOST ON FIRST TRANSIT	46.7	47.7	48.9	48.9
PERCENTAGE OF PARTICLES LOST AFTER TEN TRANSITS	77.7	77.5	79.4	80.0
PERCENTAGE OF PARTICLES INTERNALLY REFLECTED	8.3	6.8	4.0	2.1
MEAN LIFETIME OF INTERNALLY REFLECTED PARTICLES	1,334	2,005	4,567	17,792
$\xi'_{\perp\ \max}$	0.159	0.143	0.128	0.113
$\xi'_{\perp\ \min}$	0.055	0.065	0.076	0.088
T $(\xi_{\perp} - \xi'_{\perp\ \min})$	5.3	5.2	4.8	5.0

APPENDIX

MATCHING OF SQUARE-WAVE AND SINE-WAVE MODELS

Following essentially the method outlined in section 4 of L-R we can develop a similar perturbation theory of the square wave model for the first transit.

Let $r = r_o + h\, r_1 + \ldots$.

Then the equation of motion in i^{th} region can be written, to first order, as

$$v^2 \frac{d^2 r_1}{dz^2} + 4 r_1 = -2\, r_o g_i \qquad \ldots (A.1)$$

where $g_i = 0$ for $i = 0$ and $2n + 1$, and for $0 < i < 2n + 1$, $g_i = \pm 1$ according as i is even or odd, respectively. The general solution in i^{th} region is given by

$$r_{1i} = A_i \cos \left(\frac{2z}{v} + \varphi_i\right) - \tfrac{1}{2}\, r_o g_i \qquad \ldots (A.2)$$

and the phase change between any two successive boundaries is, to this order, $\theta = 2\pi/v$.

Continuity across a boundary is expressed by the equations

$$A_{i+1} \cos \varphi_{i+1} - \tfrac{1}{2}\, r_o g_{i+1} = A_i \cos (\varphi_i + \theta) - \tfrac{1}{2}\, r_o g_i \qquad \ldots (A.3)$$

$$A_{i+1} \sin \varphi_{i+1} = A_i \sin (\varphi_i + \theta)$$

$$\text{Let } X_i = \begin{pmatrix} A_i \cos \varphi_i \\ A_i \sin \varphi_i \end{pmatrix} \quad \text{and} \quad C_i = \begin{pmatrix} -\tfrac{1}{2}\, r_o (g_i - g_{i+1}) \\ 0 \end{pmatrix}$$

Initially, $X_i = 0$

In general, (A.3) can be written as

$$X_{i+1} = L(\theta)\, X_i + C_i \qquad \ldots (A.4)$$

where

$$L(\theta) = \begin{pmatrix} \cos\theta & -\sin\theta \\ \sin\theta & \cos\theta \end{pmatrix}$$

so that we can solve for X_{2n+1}, obtaining

$$X_{2n+1} = \sum_{p=0}^{2n} L^p C_{2n-p}$$

$$= r_o \left\{ \sum_{p=0}^{2n} (-L)^p \chi - \tfrac{1}{2} (1 + L^{2n}) \chi \right\}$$

where

$$\chi = \begin{pmatrix} 1 \\ 0 \end{pmatrix}$$

i.e.,

$$X_{2n+1} = r_o \left\{ (1 + L)^{-1} (1 - L^{2n}) - \tfrac{1}{2} (1 + L^{2n}) \right\} \chi \qquad \ldots (A.5)$$

This result can easily be expressed in terms of θ, but we wish simply to use (A.5) to match ξ for the square wave and sine wave at $v = 2$, for which value $\theta = \pi$ and $L = -1$. Thus.

$$\mathop{\mathcal{L}}_{L \to -1} X_{2n+1} = -2nr_o L^{2n-1} \chi = 2nr_o \chi$$

and so for the square-wave model

$$\xi = \frac{4h^2}{v^2} |X_{2n+1}|^2 = 4h^2 n^2 r_o^2 \qquad \ldots (A.6)$$

With the same value $v = 2$, and using the result previously obtained in L-R (Eqn. (4.6) with misprint corrected) we have for the sine-wave model

$$\begin{aligned} \xi &= \mathop{\mathcal{L}}_{v \to 2} \frac{8r_o^2 h^2}{(v^2-4)^2} (1 - \cos \frac{4n\pi}{v}) \\ &= \frac{\pi^2}{4} h^2 n^2 r_o^2 \end{aligned} \qquad \ldots (A.7)$$

Comparing (A.6) and (A.7), we find the values of ξ coincide if

$$h \text{ (square-wave)} = \frac{\pi}{4} h \text{ (sine wave)}. \qquad \ldots (A.8)$$

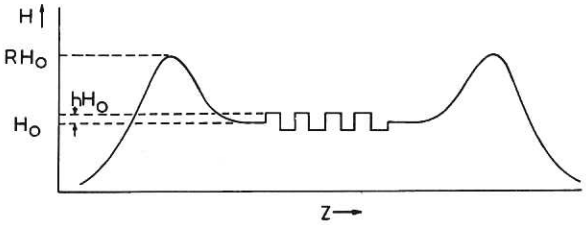

Fig. 1 (CLM-P70)
Mirror machine with 'square wave' modulation of central field

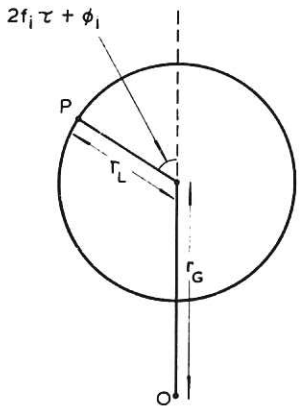

Fig. 2 (CLM-P70)
Representation of particle orbit

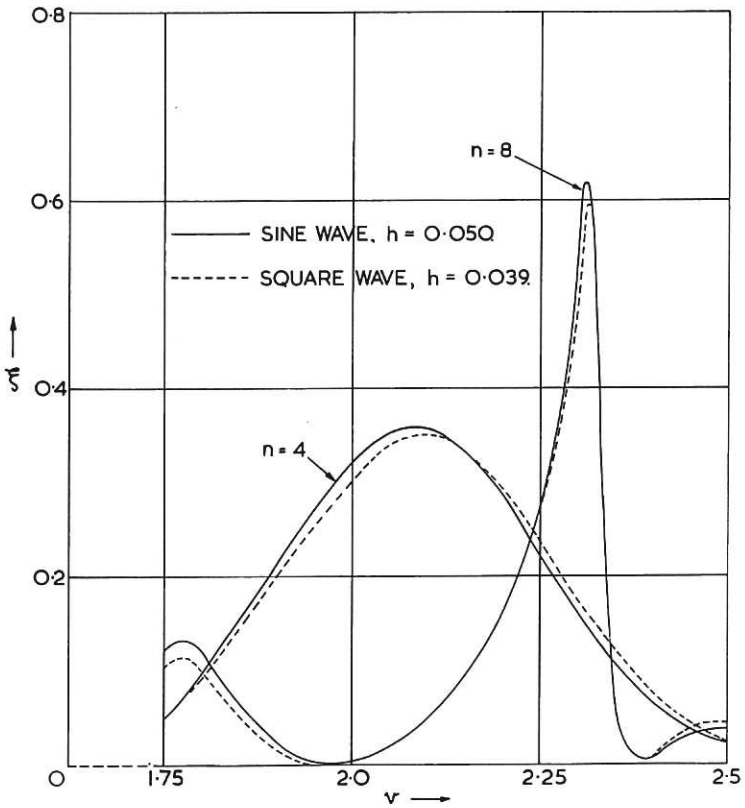

Fig. 3 ξ as a function of v, first transit (CLM-P70)

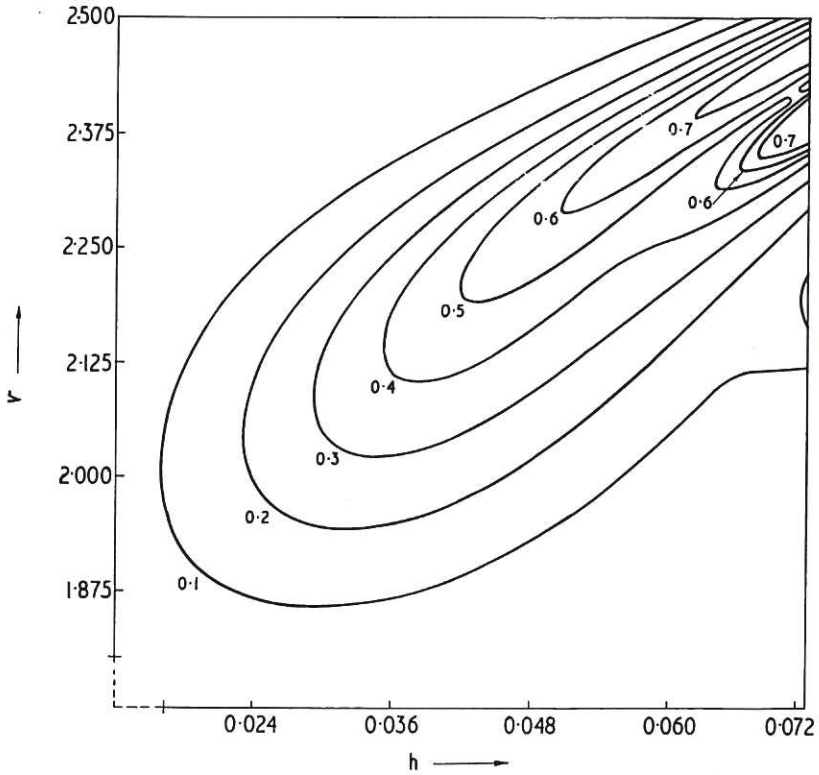

Fig. 4 (CLM-P 70)
Contours of ξ as a function of h and v, first transit
$n = 5$, $r_0 = 2$

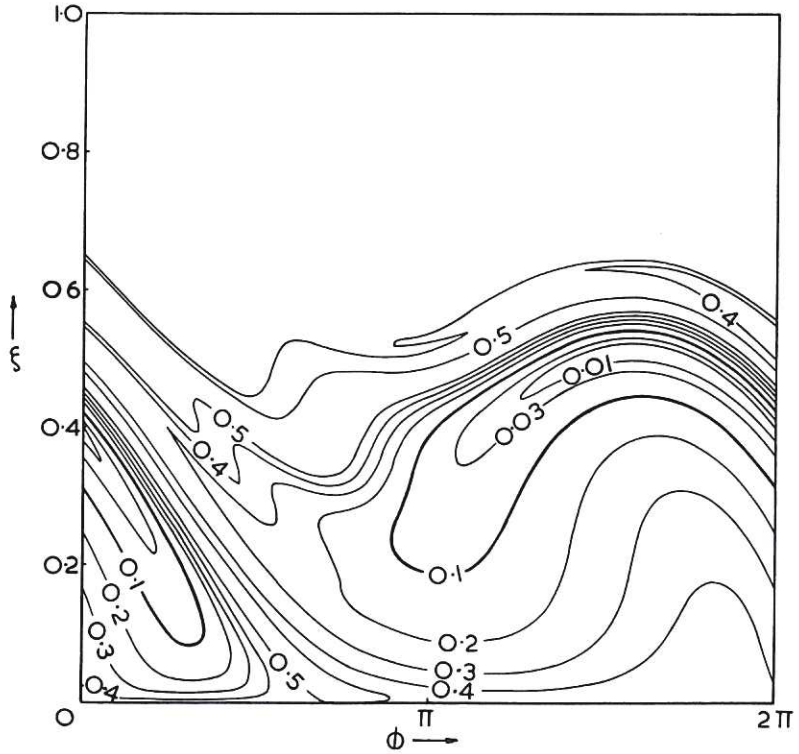

Fig. 5 (CLM-P 70)
Contours of ξ' as a function of ξ and ϕ, reverse transit
$n = 5$, $h = 0.042$, $r_0 = 2$, $v = 2.21$

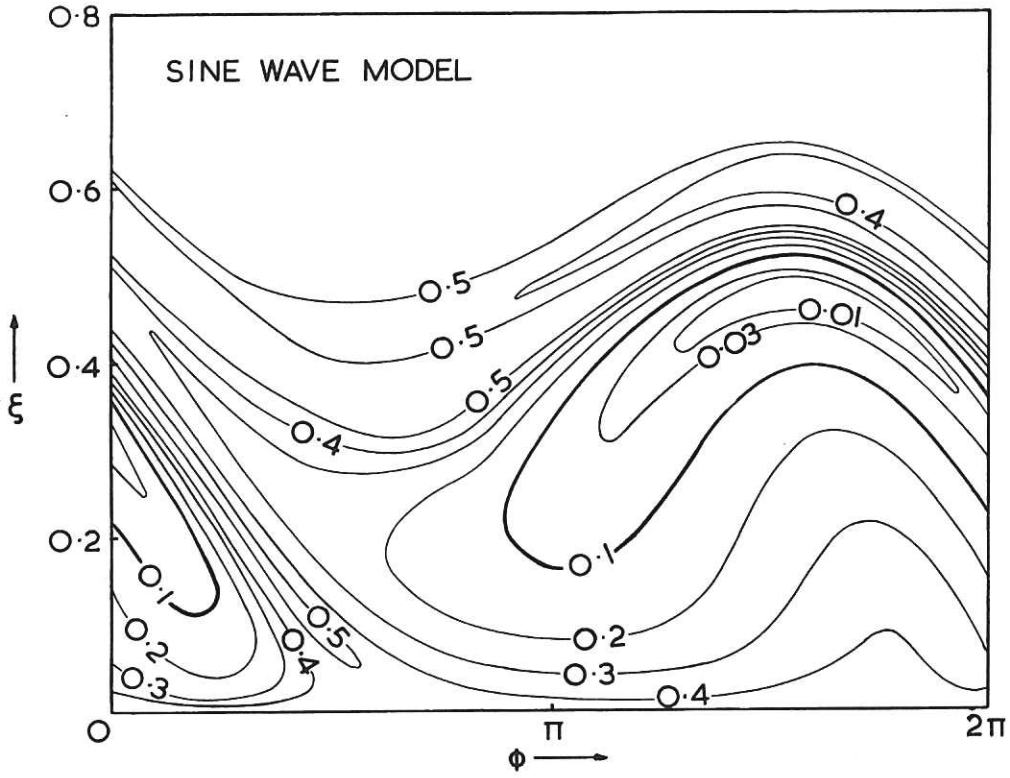

Fig. 6 (CLM-P70)
Contours of ξ' as a function of ξ and ϕ, reverse transit
n = 5, h = 0.05, r_0 = 2, v = 2.19, sine wave model

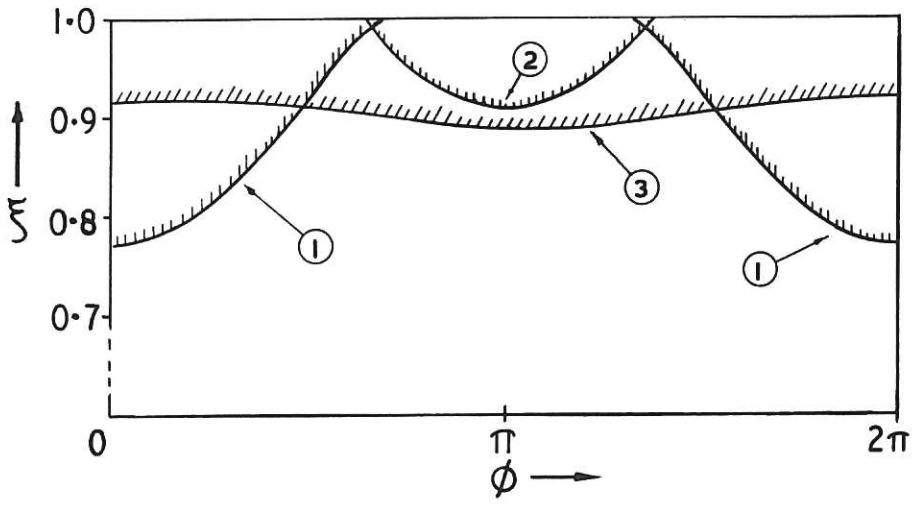

Fig. 7 (CLM-P70)
Regions of (ξ, ϕ) in which internal reflections occur at a single field step
1. 1-h → 1+h, square step h = 0.039
2. 1+h → 1-h, square step h = 0.039
3. 1-h → 1+h, cosine step h = 0.05

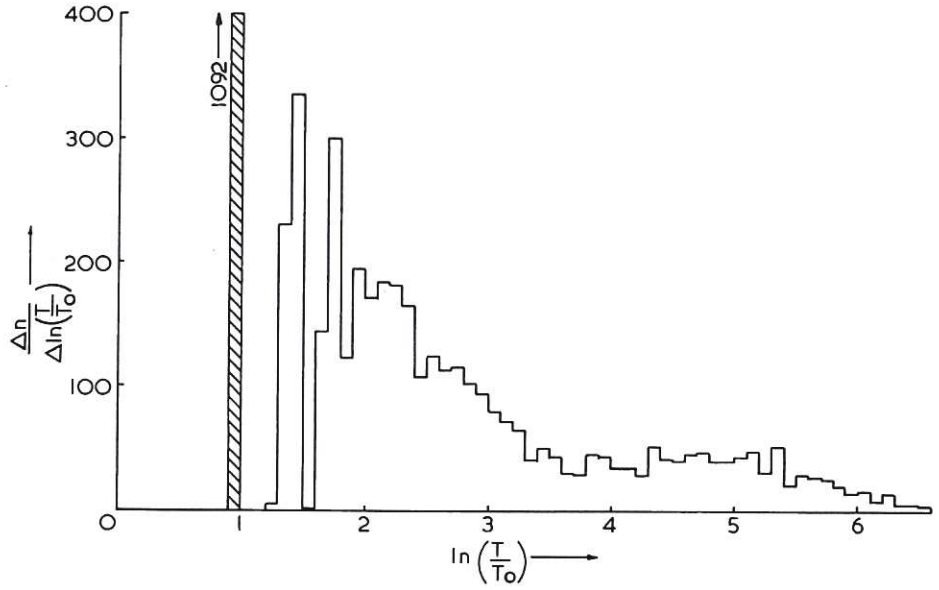

Fig. 8 (CLM-P 70)

Distribution of containment times, n = 5, h = 0.042, r_o = 2, v = 2.21

(a) Mirror ratio 10 : 1 (5000 particles)

(b) Mirror ratio 100 : 1 (1000 particles)

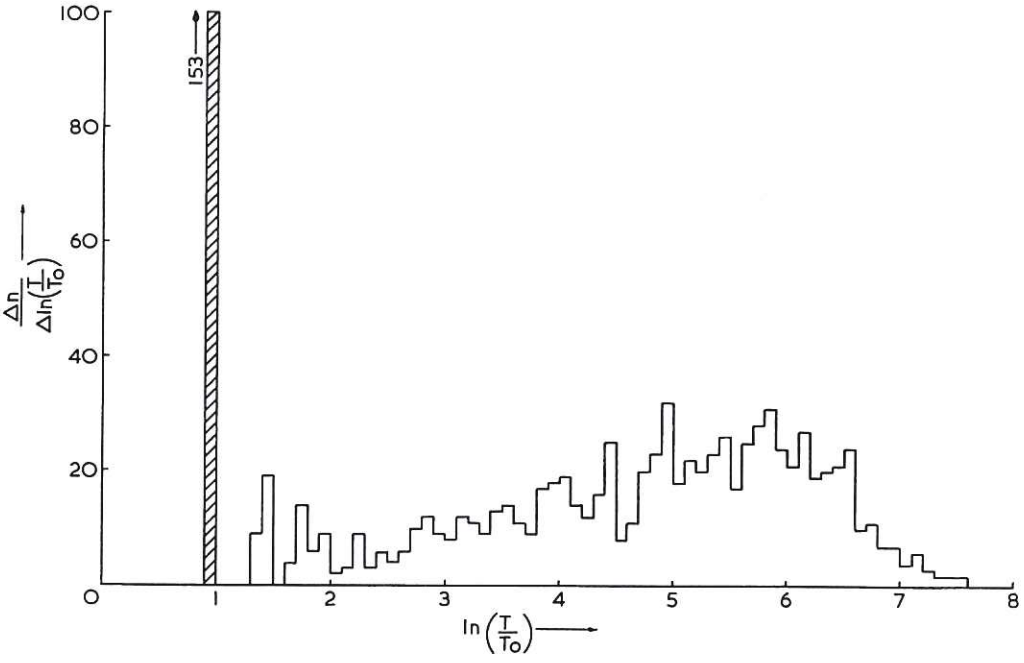

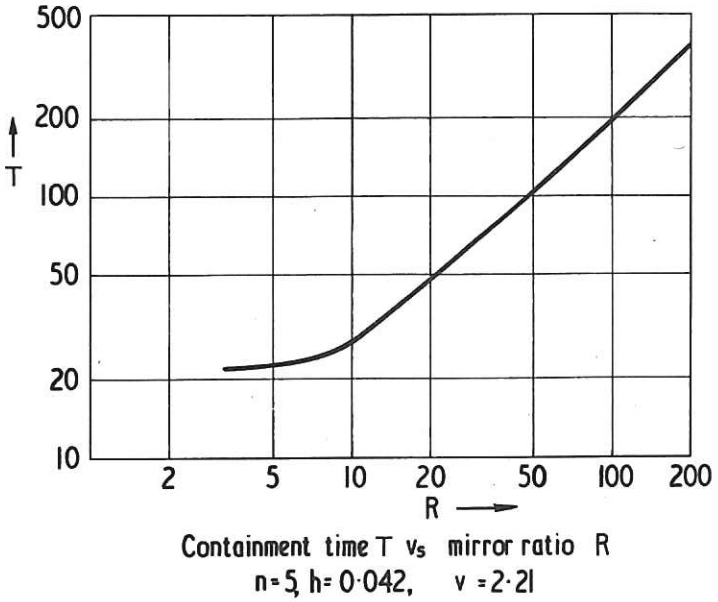

Fig. 9 (CLM-P 70)
Mean containment time T as a function of mirror ratio R

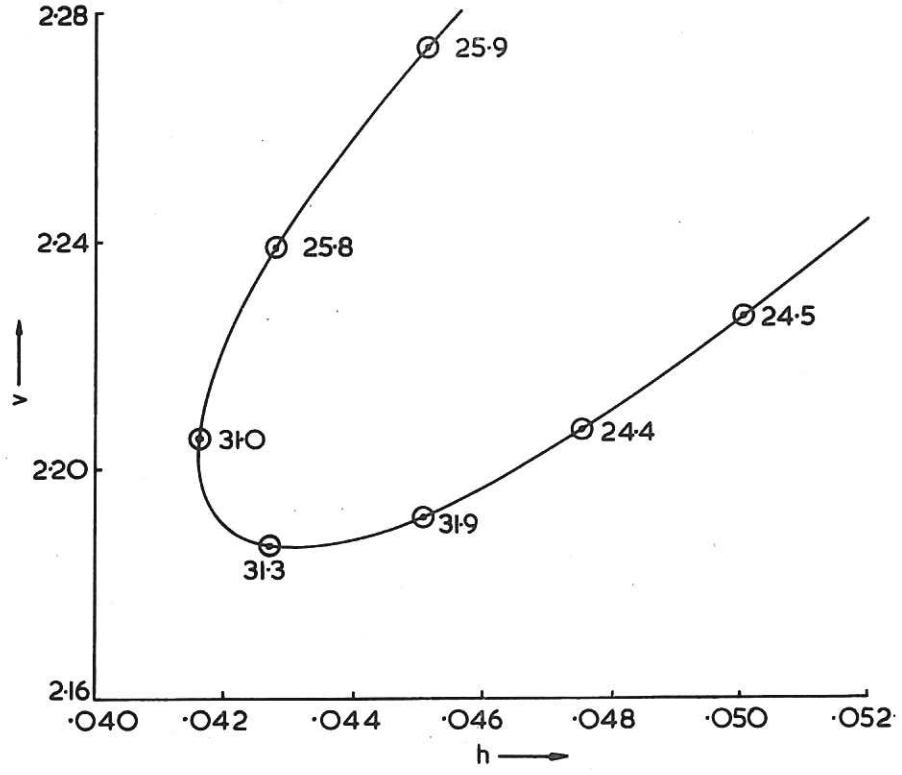

Fig. 10 (CLM-P 70)
Mean containment times plotted along $\xi_1' = 0.5$ contour

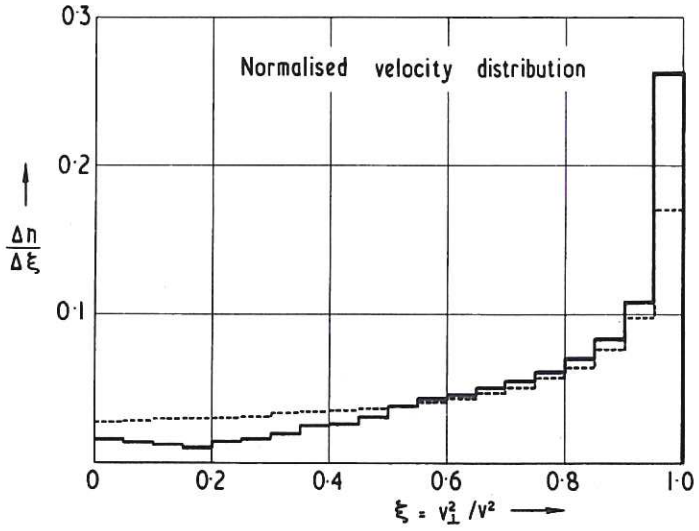

Fig. 11 Normalised velocity distribution (CLM-P 70)

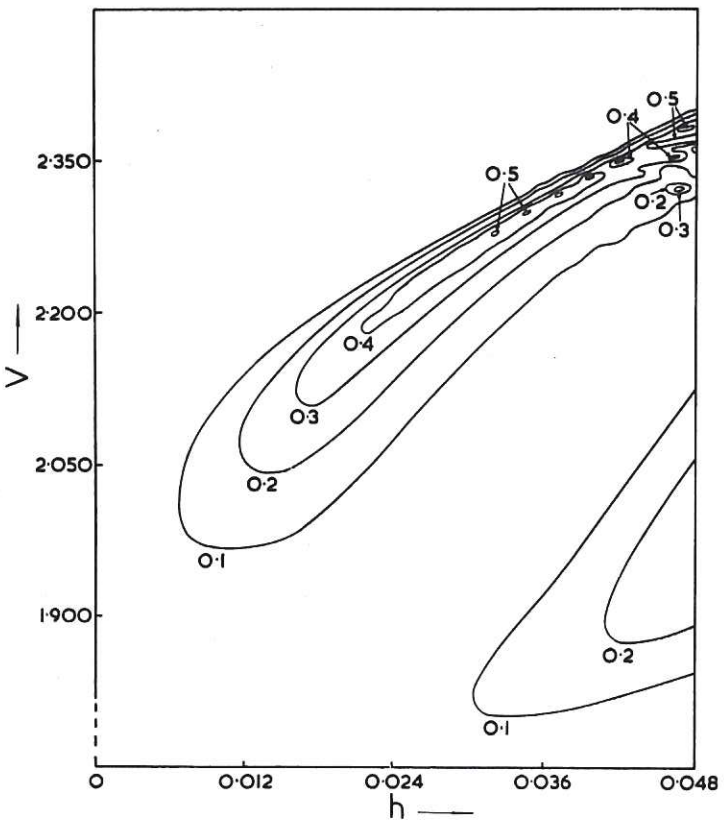

Fig. 12 (CLM-P 70)
Contours of ξ as a function of h and v, first transit
$n = 10$, $r_0 = 2$

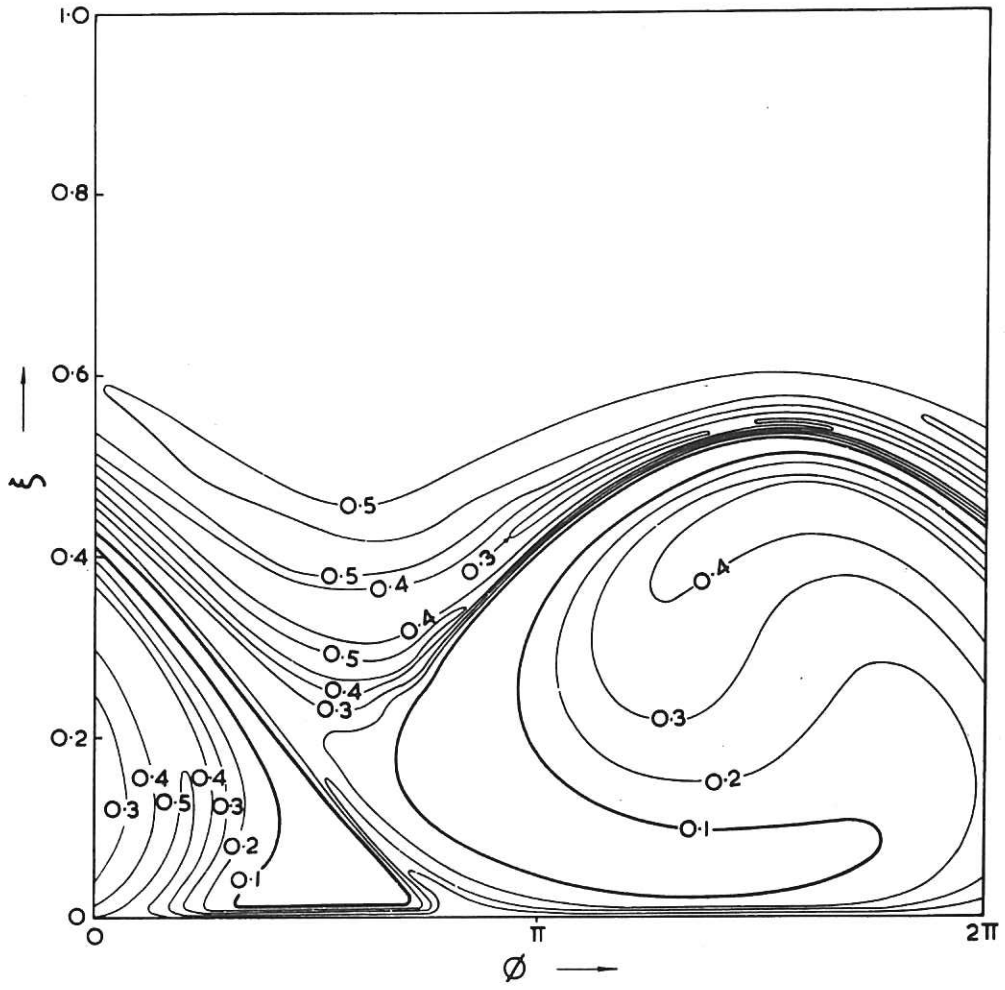

Fig. 13 (CLM-P70)

Contours of ξ' as a function of ξ and ϕ, reverse transit

n = 10, h = 0.03, r_0 = 2, v = 2.26

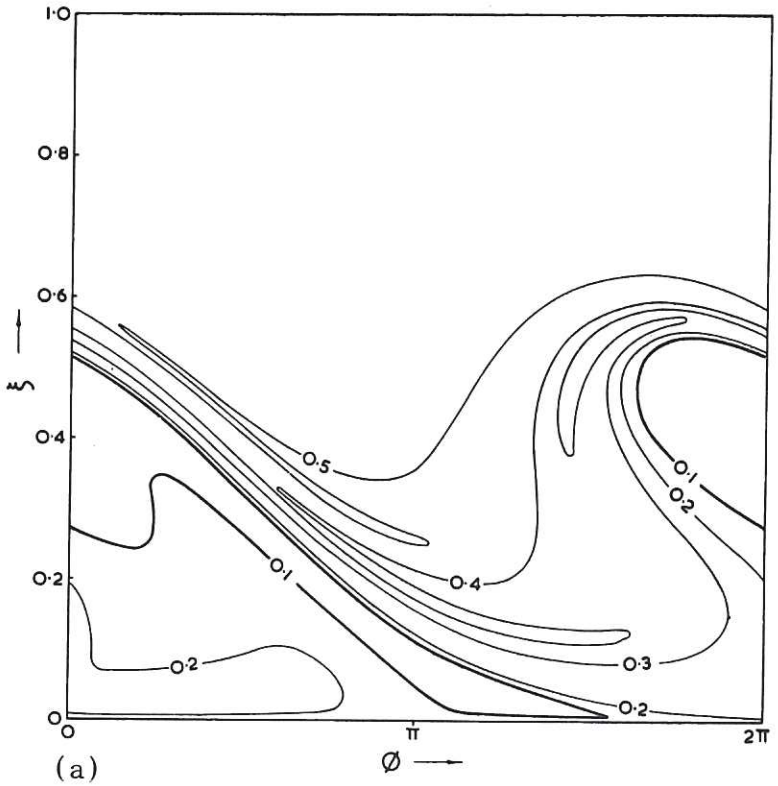

Fig. 14 (CLM-P70)

Contours of ξ' as a function of ξ and ϕ, staggered modulations $n = 10$, $h = 0.0173$, $r_0 = 2$, $v = 2$

(a) reverse transit (b) forward transit

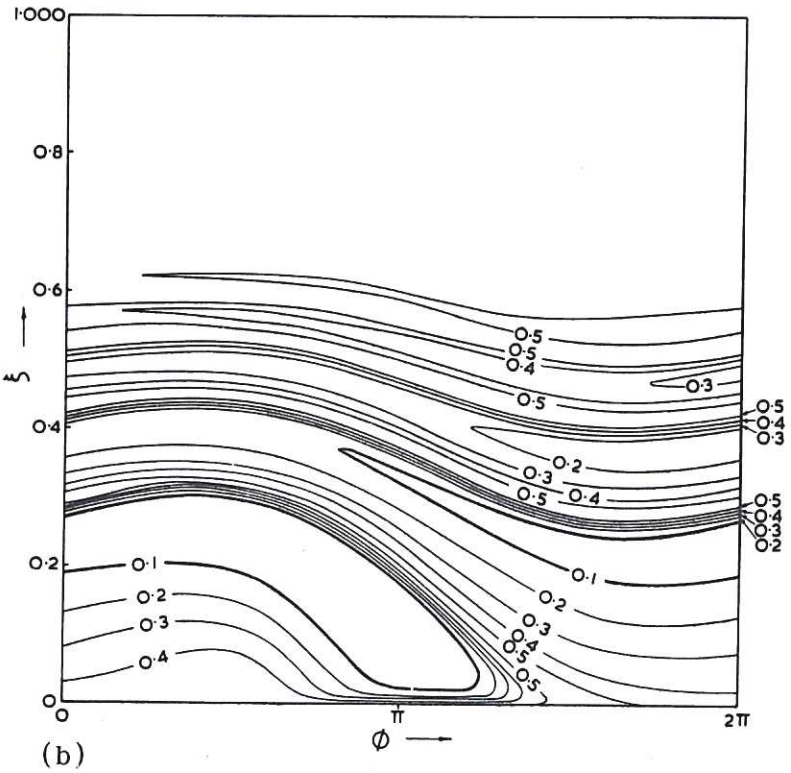

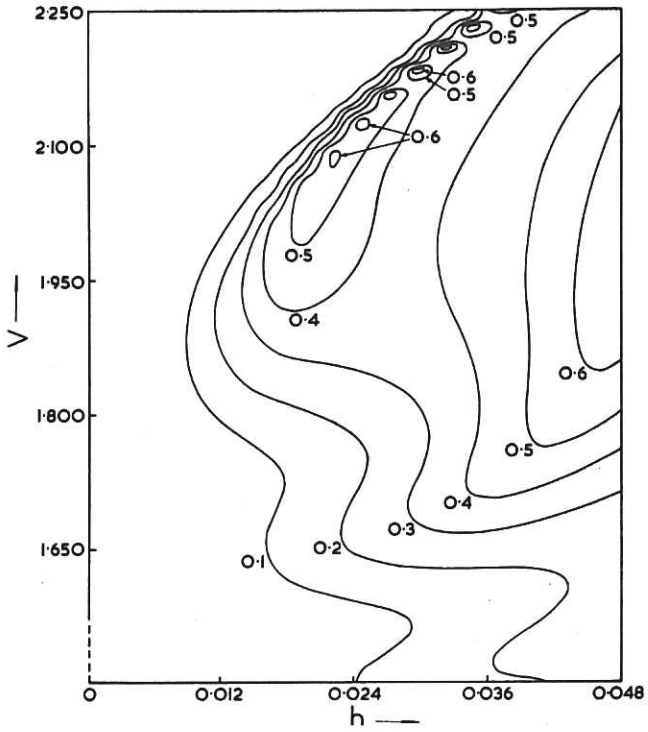

Fig. 15 (CLM-P 70)
Contours of ξ as a function of h and v, first transit
$n = 10$, $r_0 = 2$, staggered modulations

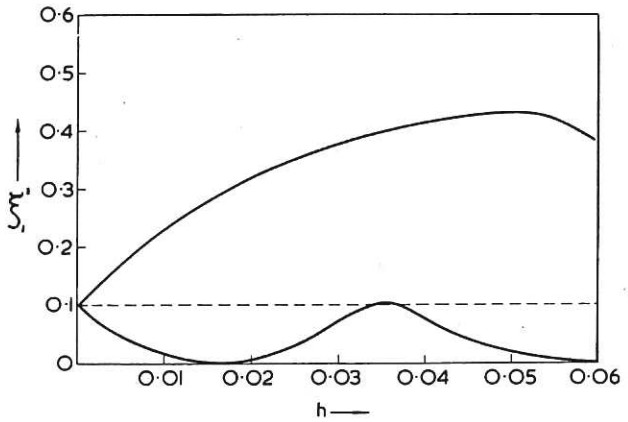

Fig. 16 (CLM-P 70)
Maximum and minimum values of ξ_1', $n = 5$,
$r_0 = 2$, $v = 2.05$, $\xi_1 = 0.1$

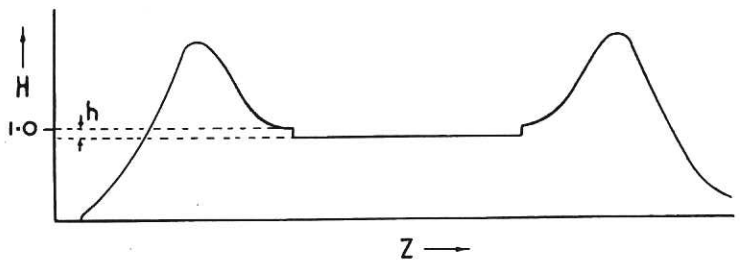

Fig. 17 Stochastic trap (CLM-P 70)